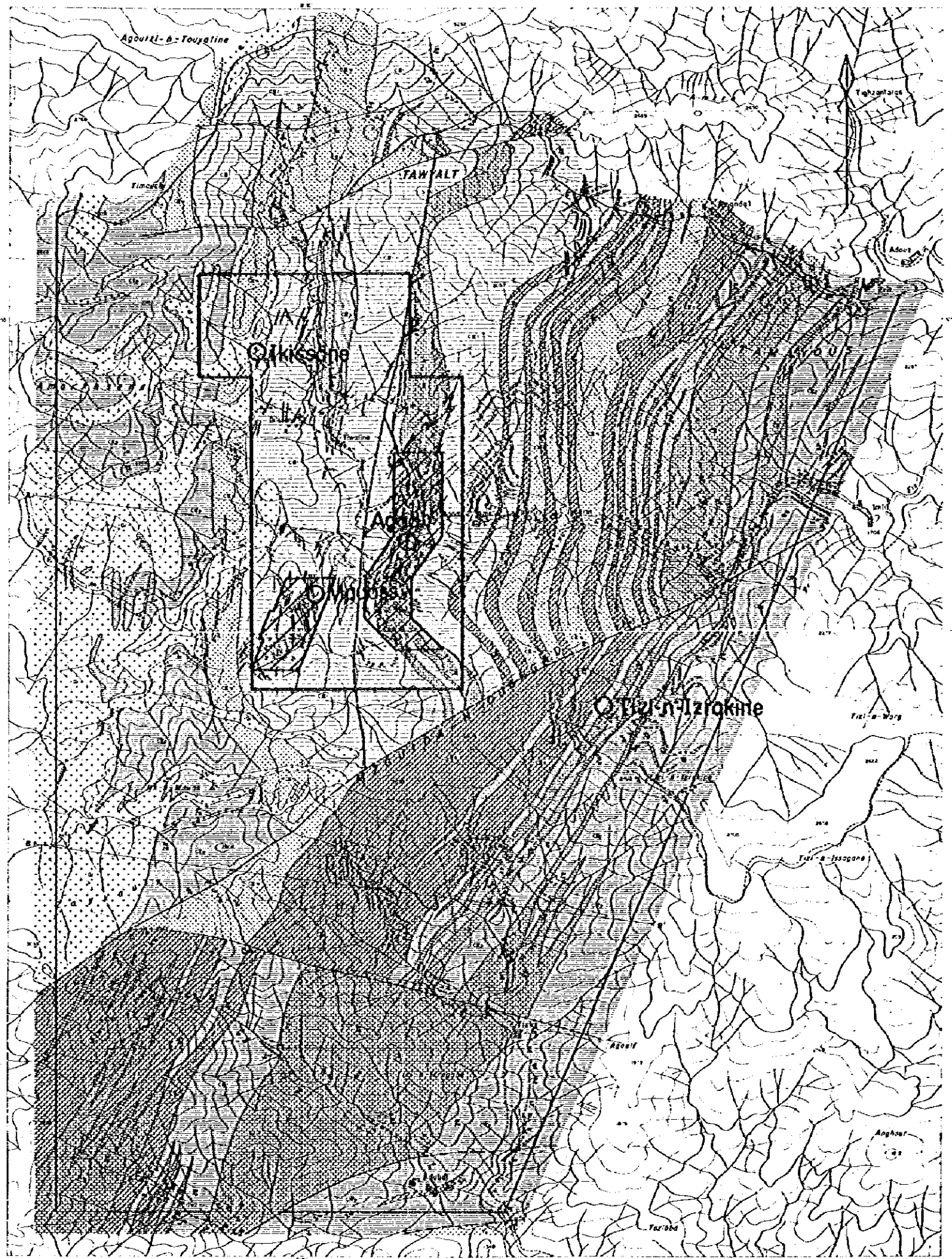


II GEOPHYSICAL SURVEY
(AGADIR SECTOR)



LEGEND

- | | | |
|----------|----|----------------------|
| Tertiary | Ts | sandstone, siltstone |
|----------|----|----------------------|
- | | | |
|---------------------|---------------|--|
| Ordovician-Cambrian | CIV Formation | CIVp pelitic schist |
| | CII | CII limestone |
| | CIIa | CIIa calcareous schist |
| | CII Formation | CIIp pelitic schist |
| | CIIb | CIIb psammitic schist |
| | CIIc | CIIc green schist (tuff, tuff breccia) |
- | | | |
|---------------|------|----------------|
| CII Formation | CIIp | pelitic schist |
|---------------|------|----------------|
- | | | |
|-----------------|----|------------|
| Intrusive rocks | Gr | granite |
| | Po | porphyrite |
| | Ap | aplite |
| | sk | skarn |
- | | |
|---|---------------|
| / | fault |
| | bedding plane |
| ~ | cut |
- | | |
|-----|----------------------|
| [] | magnetic survey area |
| / | IP survey area |
- | | |
|---|----------------------------------|
| ○ | ore deposits
mineral showings |
|---|----------------------------------|

Fig. II-1 Geophysical Survey Area

CHAPTER 1 MAGNETIC SURVEY

1-1 Outline of Magnetic Survey

1-1-1 Outline of Magnetic Survey Method

The rocks of earth's crust have their own individual magnetism, depending both on their containing magnetic minerals and amounts. And this magnetism usually creates both induced magnetization which is caused by the earth's magnetic field, and remnant magnetization depending on each individual rock. Magnetic fields created by the said magnetism are very small in comparison with the normal magnetic field of the earth, but they can be detected as magnetic anomalies by reducing the normal magnetic field from the measured magnetic field.

In general, the intensity of rock magnetism varies in proportion to its magnetic susceptibility (K). And the susceptibility (K) depends upon the amount of the magnetic minerals contained in each rock. In most cases, igneous rocks are higher in magnetic susceptibility than either sedimentary or metamorphic rocks. And among igneous rocks, basic rock being higher than acidic rock in susceptibility.

Then, magnetic survey can be defined as a method to infer the distribution of rocks, as well as the regional geological structures, by means of detecting the difference of magnetic features of rocks.

In the surveyed Agadir Sector, it has been proved by the second year's geological survey that the skarn zone was formed in limestone by the intrusion of granite, and in some part of the skarn zone mineralization was also formed. Considering the presence of pyrrhotite with strong magnetism in the mineralization zone, magnetic anomalies must be detected if the mineralized zone occurs in massive form. Based on these reasons, the current magnetic survey was undertaken to know the relations of magnetic distribution with both geological structure and the distribution of mineralized zones.

Generalized survey process from the field measurement to the completion of the survey report can be shown as a flow chart, Fig. II -1-1.

1-1-2 Field Survey

The survey area is located between 1,800m and 2,600m in altitude, and mostly covered by steep mountains. The geology of the area is consisted of rich distribution of schists with 400m wide limestone in the eastern part of the area which elongates from north to south, and numbers of large and small intrusion of granite are also observed in the area, as shown in Fig. II -1-2.

1) Survey stations and base station

The magnetic survey was done in a area of 4 km by 2 km as shown in Fig. II -1-2, and the measurement was carried out in the following 520 stations which were also used for both geological and geochemical survey. After setting the base station at the western edge of the Agadir village, observation of diurnal variations of the earth's magnetic field was regularly undertaken during the magnetic survey period.

- Whole survey area: 220 measurements with survey interval of about 100 m, selected from the survey route along major local streams.

- Grid survey area: 300 measurements with survey interval of about 50 m, along east-west survey lines.

(The grid survey area was more important area, and total 30 survey lines of about 450 m long were set in 100 m intervals which generally intersect the strike of the formation rectangularly.)

At these survey stations, the magnetic measurements were done more than

three times, respectively, and the observed mean values were adopted as of the magnetic survey value. The variation of the measured values was as small as less than 10 nT.

2) Survey Instrument

The adopted major instruments were as follows.

(1) Field survey

- Proton magnetometer: Type G846, EG&G Geometrics, sensitivity 1nT(γ)

(2) Base station observation

- Proton magnetometer: Type G806, Geometrics, sensitivity 1nT(γ)

- Pen recorder: Type EPR-100A, Toa Electronics Ltd. sensitivity 1mV/7.5cm

1-1-3 Data Processing Method

1) Diurnal correction

In general, the magnetic field of a survey station varies both by sudden magnetic storms, which appear in irregular and radical changes, and yet by rather regular changes on a daily cycle basis. For these reasons, diurnal correction of each magnetic measurement becomes necessary depending on the recorded time of the measurement.

Fig. II-1-3 and II-1-4 are the observation results of the base station. The observed diurnal amplitude ranges approximately between 10nT and 50nT, and no magnetic storm has been recognized so far which shows remarkable magnetic changes.

In order to correct the diurnal changes, the value of 39,780 nT observed on July 1, 1985 at the base station was selected for the basic magnetic intensity.

The diurnal variation corrected magnetic intensity of each survey station can be calculated by the following equation,

$$R_s = \overline{R_{st}} + \Delta R_t = \overline{R_{st}} + (39,780 - R_{bt})$$

where, R_s : Diurnal variation corrected magnetic value

$\overline{R_{st}}$: Average of measured values of each survey station at a time of t

R_{bt} : Magnetic value of the base station at t

ΔR_t : Diurnal correction value at t

The observed values of the base station are shown in Table II-1-1 at the end of the report.

2) Drafting of total magnetic intensity map

Total magnetic intensity map was drafted by plotting the distribution of magnetic intensity which were calculated by reducing the normal magnetic field from the diurnal variation corrected magnetic values R_s of respective survey stations. Because of the fact that the survey area was so small as 2 km by 4 km, normal magnetic field was reasonably considered as a definite one. Then, the normal magnetic field of the survey area was assumed as of 39,900 nT after analyzing the measured field data.

Meanwhile, the drafting of the total magnetic intensity map was undertaken in the following procedures. That is, first of all, to make a compiling draft map out of field data R_s , and then to read out the magnetic values of each grid intersection which depends on a mesh of 50 m by 50 m. Then, those magnetic values of each grid intersection are read and put into a computer, and the intensity map is drafted by a plotter after the normal magnetic field is withdrawn.

3) Trend surface analysis

In order to detect the trend of regional magnetic variations observed

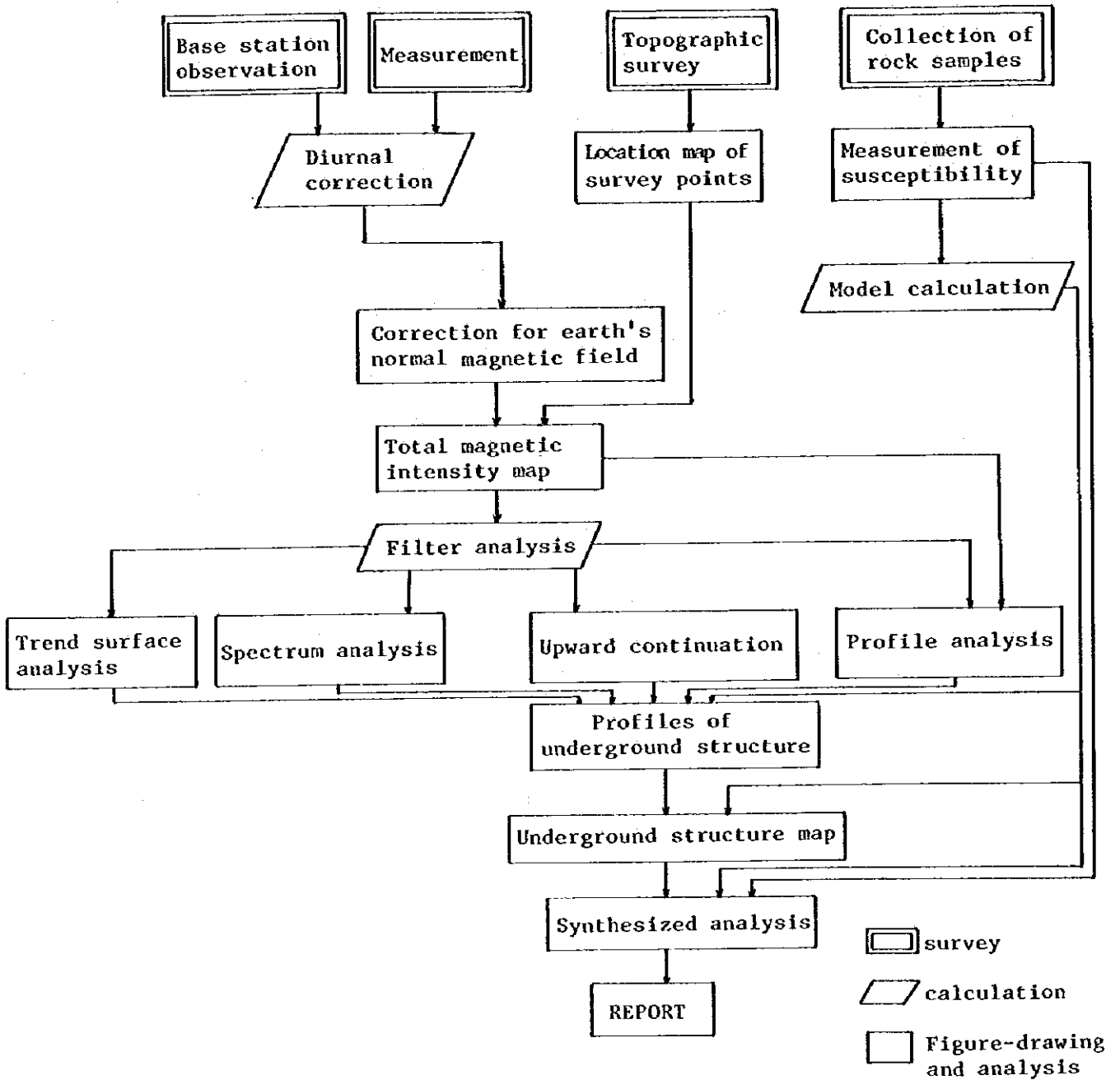
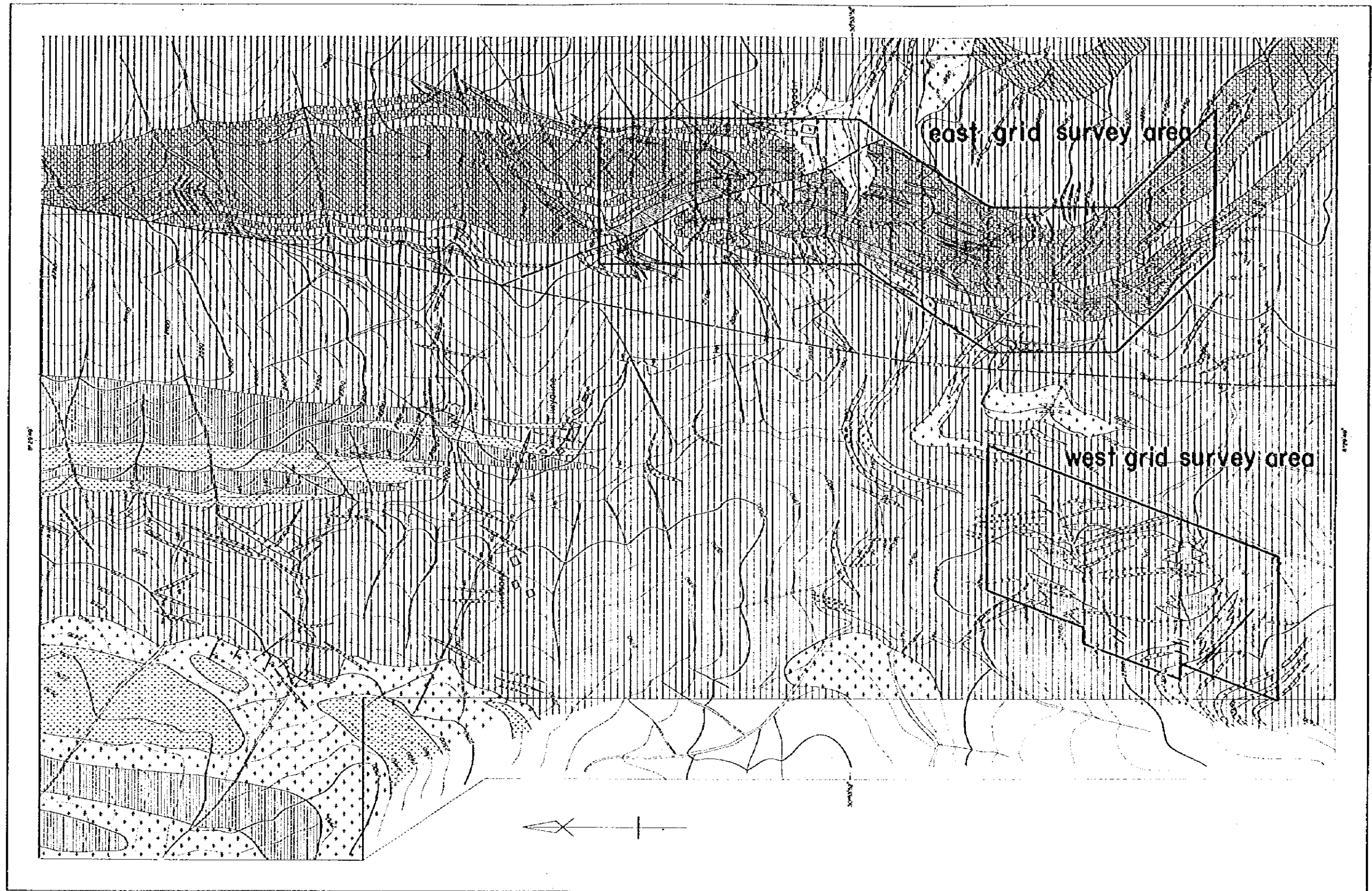
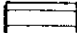
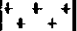
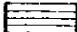

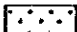

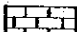
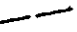
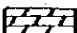



Fig. II-1-1 Flow Chart of Magnetic Survey



LEGEND

- | | | | |
|---|-----------------------------------|---|------------|
|  | green schist (tuff, tuff breccia) |  | granite |
|  | pelitic schist |  | porphyrite |
|  | psommitic schist |  | skarn |
|  | limestone |  | fault |
|  | calcareous schist |  | ore vein |


S=1:12,500
 0 500m

Fig. II-1-2 Location Map of Magnetic Survey Area

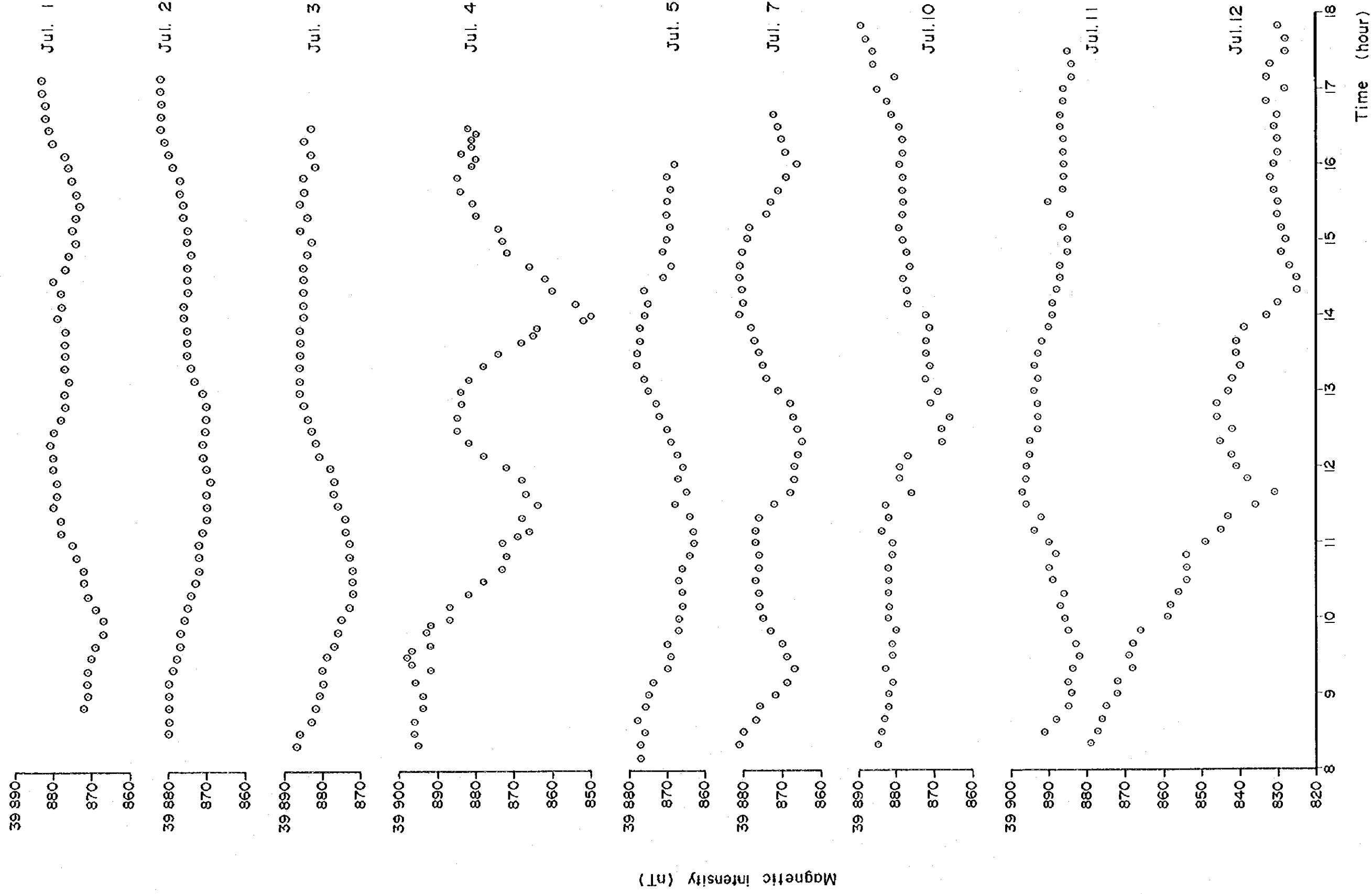


Fig. II-1-3 Diurnal Variation of Geomagnetic Field at the Base Station

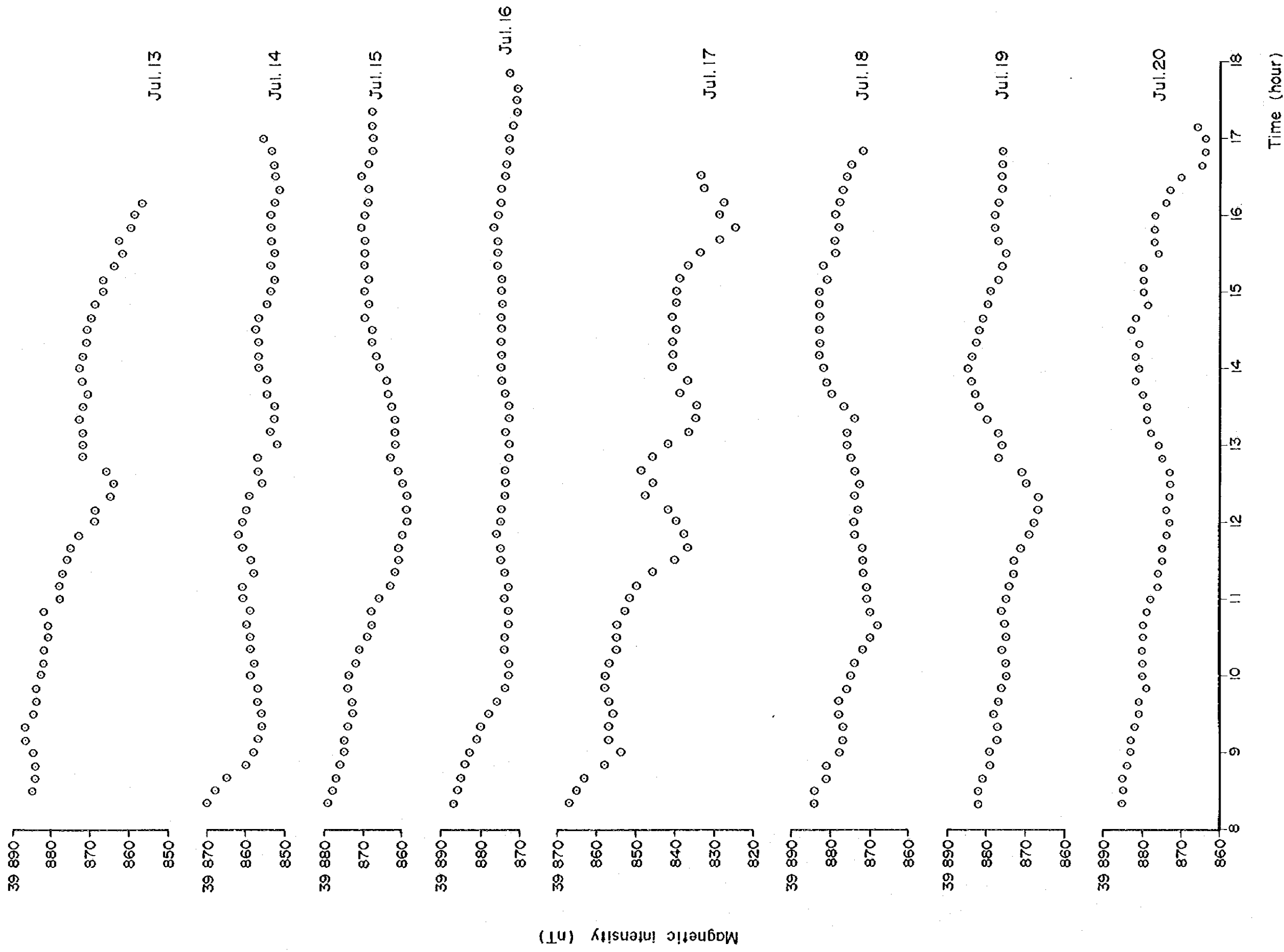


Fig.II-1-4 Diurnal Variation of Geomagnetic Field at the Base Station

in the total magnetic intensity map, the trend surface in third order polynomial was analyzed. This was done by approximating the total magnetic intensity map through a three dimensional curved surface arranged by the following equation, which was calculated by least square method using the surveyed magnetic values at respective grid intersections.

$$Z(x,y) = -0.3048 - 17.079x - 5.6735y + 0.72583x^2 + 0.30784xy \\ + 0.1488y^2 - 0.007832x^3 - 0.003422x^2y - 0.002594xy^2 \\ - 0.00106y^3$$

4) Drafting of upward continuation map

Upward continuation map shows such an effective usage as one obtained by an airborne survey. In other words, it reduces the short wavelength (high frequency) anomaly caused by minor structures near the ground surface, and renders the longer wave magnetic anomaly become dominated. This fact makes it easier to detect some larger characteristics of a magnetic survey map.

Upward continuation map (projected at 50 m level above the ground) was drafted by multiplying the grid magnetic values of a total magnetic field with upward continuation coefficients by means of convolution method.

5) Spectrum analysis

Total magnetic intensity map contains waves of different wavelength based on miscellaneous factors. The spectrum analysis is a method which separates shallow structures from deeper structures by the length of the short waves.

Spectrum analysis map shows the distribution of logarithmic values of energy spectrum $\log E$ at various frequency levels called f . If we assume that f_x as of X directional frequency, f_y as Y directional frequency, and $S(f_x, f_y)$ for a complex spectrum regarding both amplitude and phase of the wave, then we can calculate the energy spectrum E as a function of these figures.

Fig. II-1-5 shows a spectrum analysis map, and it gives a set of approximated two straight lines from the distribution of the logarithmic energy spectrum $E(f)$. In reading the gradients of these regression lines, the average depth $H(m)$ of anomaly sources, which cause the magnetic anomaly, can be calculated by the following equation,

$$H = - \frac{1}{4\pi} \cdot \frac{\Delta \log E}{\Delta f}$$

In analyzing by the method, the magnetic structures of the current survey area have been roughly classified into two categories, that is, a regional component with average depth of 760 m and a near surface component with average depth of 80 m.

In addition, a regional component analysis map was drafted by means of convolution of both weighting function, which was separately calculated by the factors read from the spectral analysis map, and magnetic intensity at the grid intersection involved.

6) Model calculation

The response of a magnetic body varies very much depending on three magnetic elements (total magnetic intensity, declination and inclination), and then it becomes necessary to clarify their characteristics based on respective survey areas. Consequently, two-dimensional model calculations were done on both dyke and step models in changing the declinations from magnetic north and inclinations.

The results are shown in Fig. II-1-6, where the depth of the underlying model, the inclination of dykes, the strike of the structure activate the change of magnetic distribution which appears in a profile vertical to the strike of the structure. In case $\alpha = 90^\circ$, the magnetic distribution in east to west profile is illustrated where the magnetic body lies in north to south direction.

In the survey area, the north to south oriented geological structures are dominated, then the model under $\alpha = 90^\circ$ is considered suitable for analysis. From the calculation results of these models, in case of dyke structures in the region, two types of positive anomalies are to be considered, that is, one with relatively small scale and the other of steep gradient with a small scale negative zone on its one side. In case where the inclination of the dyke is different, the magnetic distribution becomes reverse in its position. (see Fig. II-1-6, (5) and (6))

7) Profile analysis

Two-dimensional profile analysis was done for the selected four profiles shown in the total magnetic intensity map. The profile analysis is done as follows,

- (1) Magnetic profile is drafted from the total magnetic intensity map at first, and the magnetic values read from the profile are put into a computer after removing the regional trend influence from the data in consideration of the filter analysis results.
- (2) To make an underground structural model, and put the data into the computer, after considering the geological information, the susceptibility of rocks and the results of model calculations, then the magnetic response on the surface is calculated.
- (3) In comparing the calculation results and the magnetic intensity data, the underground structure model will be automatically changed of its position, shape, and susceptibility, and the magnetic response will be re-calculated.
- (4) In case when a good coincidence being not obtained after taking those procedures stated above, the researcher would generally re-input necessary data to the computer after redesigning a new underground structure model by adding the aforementioned calculation results.

By repeating the procedures of above-stated (3) and (4), an underground structure model can be obtained which shows good calculation results coinciding well with input magnetic values. However, there might be theoretically infinite numbers of underground structure models which could show the same values on the magnetic profile. Consequently, utmost attentions should be necessarily paid for a reasonable coincidence between the geological structure model obtained by the said calculations and the actual geological information.

1-2 Results of Magnetic Survey

1-2-2 Analytical Maps of Magnetic Survey

Based on the results of the analysis, the following maps were drafted.

- PL. II -1-2 Total Magnetic Intensity
- PL. II -1-3 Magnetic Trend (Third Order Polynominal)
- PL. II -1-4 Upward Continuation of Total Magnetic Intensity
- PL. II -1-5 Deep Magnetic Component
- PL. II -1-6 Results of Magnetic Modeling
- PL. II -1-7 Magnetic Profile with Geological Structure

Characteristic notifications observed on these maps are summarized as

LOGARITHMIC ENERGY SPECTRUMS

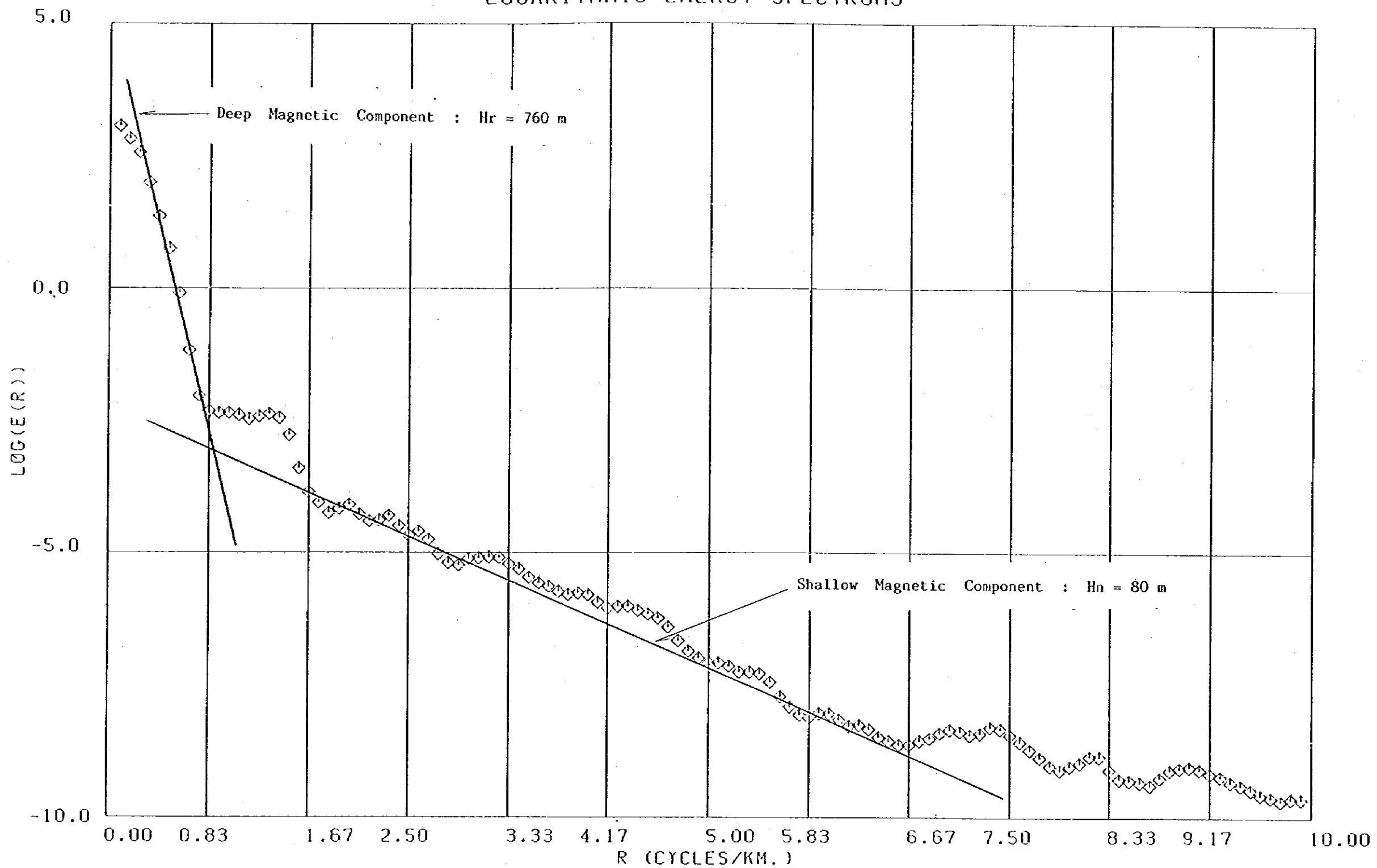


Fig. II-1-5 Spectrum Analysis

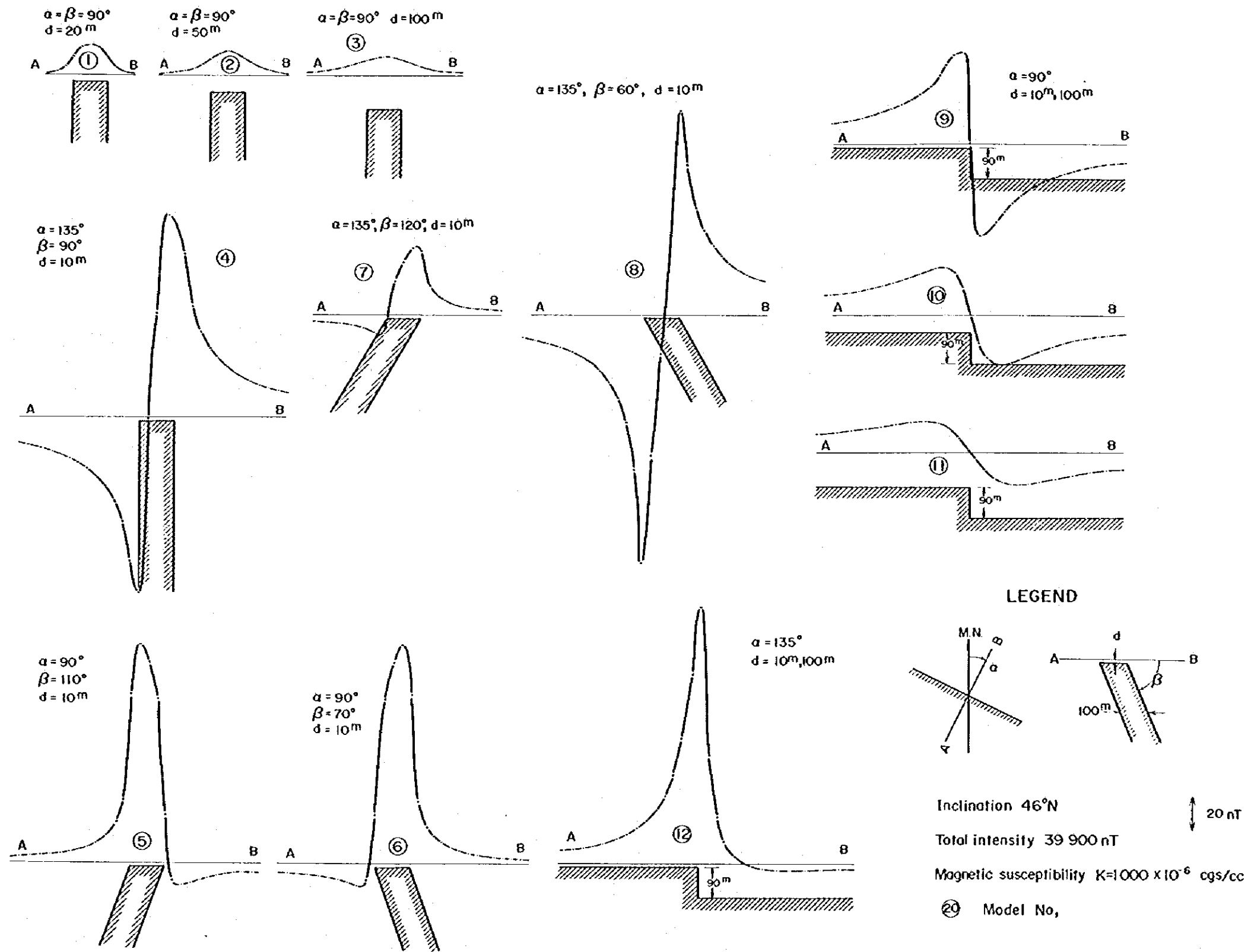


Fig. II-1-6 Magnetic Response of Dyke and Step Model

follows.

1) Total magnetic intensity (PL. II -1-2)

(1) Iso-magnetic contours display a pair of elongating tendencies, north to south and northeast to southwest directions. As a general feature, the variation of magnetic values is small in the northern part of the survey area, while it is large in the central and southern part to make a contrast.

(2) There are numerous high and low anomalies with shorter wavelength in the grid survey area. The size of the respective anomalies ranges approximately from 50 m to 100 m in outer diameter with magnetic amplitude of about 50 nT to 200 nT. However, the anomalies are less in numbers and smaller in scale in the southeastern part of the survey area. Out of these anomalies, there are other smaller anomalies in overall survey area, which present distorted contours in appearance.

(3) In the external part of the survey area, there are three remarkable anomalies which have large wavelength and also amplitude.

- The northern area: Both high and low anomalies are found around the survey station, No. 323

- The central area: Both high and low anomalies observed around the survey station, No. 394

- The southern area: Both high and low anomalies around the survey station, No. 439

(4) Regarding the variations of the magnetic field, the largest was observed in the anomaly near the topographical base point (Station, No. 394). And it ranges between the minimum of $-440(+39,900)$ nT and the maximum of $390(+39,900)$ nT.

2) Magnetic trend (PL. II -1-3)

(1) Iso-magnetic contours generally present NNE to SSW directional arrangement except in the southern part of the area. The magnetic intensity becomes higher toward the eastern area uniformly, and increases so much as 125 nT in total.

(2) In the south of the Agadir village, the iso-magnetic contours change into east to west direction, and gradually reduces their magnetic intensity. The reduction amounts to 125 nT in total.

3) Upward continuation of total magnetic intensity (PL. II -1-4)

In general, the upward continuation map resembles the deep magnetic component map which will be introduced subsequently. However, the upward continuation map is thought to reflect the deeper structures better, because the numbers of magnetic anomalies are decreased in it. In other words, those short wavelength anomalies observed often in the total magnetic intensity map deplete more than the deep magnetic component map, and even disappear in the upward continuation map. Nevertheless, in the current survey, those long wavelength anomalies detected in the total magnetic intensity map remain as large scale anomalies in the upward continuation map.

4) Deep magnetic component (PL. II -1-5)

(1) Either those small amplitude anomalies in short wavelength, which are seen often in the total magnetic intensity map, or other anomalies found with distorted contours have depleted and almost become unrecognized, however, the anomalies with longer wavelength and also larger amplitudes still remain to be observed in the deep magnetic component map.

(2) Those anomalies distributed close to close in the total magnetic intensity map are often expressed to be a single anomaly.

(3) Though it was obscure at first on the total magnetic intensity map for the overlapping influence of other typed anomalies, a large scale anomaly has been clearly detected in the south-western corner zone of the survey area.

(4) Iso-magnetic contours have been found, in trend, to make a north to

south oriented arrangement in the area running from north-east to south-west part of the current survey area.

5) Results of magnetic modeling (PL. II -1-6)

By calculating the profile model on the typical magnetic anomalies appeared on the four profiles shown on the total magnetic intensity map (PL. II -1-2), models of magnetic bodies have been made.

Magnetic anomalies was well explained on dyke models, and the difference of magnetic susceptibility between the model and the near-by rock formations has been estimated as of $(1,200 \text{ to } 9,000) \times 10^{-6}$ cgs/cc, $3,200 \times 10^{-6}$ cgs/cc in average.

6) Magnetic profile with geological structure (PL. II -1-7)

Regarding the aforementioned four profiles, all of which almost rectangularly intersect the strike of the formations, a structural model has been drawn based on the results of the total magnetic intensity, filtered magnetic data, inferred geological profiles, and the results of magnetic modeling. Respective locations of the four profiles are shown in the total magnetic intensity map.

(1) Short wavelength anomalies of 100 to 300 nT are observed in the eastern (right-hand) side of the profiles, namely B-B' and C-C'. These anomalies can be reasonably explained to be of dyke models, each of which has a width from 50 m to 90 m and a length of over 100 m, and their inclinations are either vertical or steeply dipping toward the east. Susceptibility of the magnetic bodies has been estimated as of $1,300 \text{ to } 4,700 \times 10^{-6}$ cgs/cc. These models present a good correspondence with the distribution of skarn minerals as shown in the geological profiles.

(2) The magnetic anomaly detected at the western edge (left corner) of the D-D' profile led to an interpretation that there is a short wavelength anomaly in the west of the long wavelength anomaly. And the short wavelength anomaly was explained as of a steeply inclined dyke model, which has been inferred to correspond with a vein type mineral deposit in the geological profile.

(3) However, the relations of both other anomaly of large scale and the magnetic model inferred by the said anomaly with the geological structure have not been made clear as yet.

1-2-2 Magnetic Susceptibility Measurements of Rock Samples

- Measuring instrument: Bison Instruments, type 3101 susceptibility meter, the range of measurement 10^{-1} to 10^{-6} cgs/cc.

Twenty-three pieces of typical rock samples distributed in the survey area were measured of their specific susceptibility after being ground by a non-magnetic mill into 2 mm to 3 mm diam. grains, the result of the measurement is presented in both Table II-1-2 and Fig. II-1-7. From the measured result, the following facts have been clarified.

1) Both limestone and granite show such low magnetic susceptibilities as of 33×10^{-6} and 56×10^{-6} (cgs/cc), respectively. These rock samples have a common characteristics, that is, the measured magnetic susceptibilities have low variations among the rock samples.

2) Porphyrite has shown a little higher susceptibility of 77×10^{-6} cgs/cc in average, and its variation among the samples was as low as those of limestone and granite.

3) As shown in Fig. II -1-7, schists have been found consistent of two groups in terms of susceptibility, that is, low group of 52×10^{-6} cgs/cc in average and high group of 860×10^{-6} cgs/cc. And also, skarn zone shows both low and high magnetic susceptibilities, place to place.

Table II -1-2 Results of Magnetic Susceptibility Measurements

Sampling Site (Station No.)	Rock Type	Specific Susceptibility ($\times 10^{-6}$ cgs/cc)
30	green schist	840
103	green schist	91
209	green schist	33
240	green schist	784
284	green schist	48
393	green schist	967
458	green schist	62
E	green schist	56
F	green schist	39
average of 8 samples		(132)
44	limestone	36
68	limestone	30
average of 2 samples		(33)
87	granite	24
339	granite	55
495	granite	46
average of 3 samples		(39)
47	porphyrite	35
334	porphyrite	88
406	porphyrite	147
average of 3 samples		(77)
82	skarn	87
G	skarn	866
average of 2 samples		(274)
A	ore	437
B	ore	100
C	ore	27400
D	ore	1560
average of 4 samples		(1169)

A, B, C, D, E, F and G are rock sampling sites without magnetic measurement. Their locations appear in PL. II -1-1.

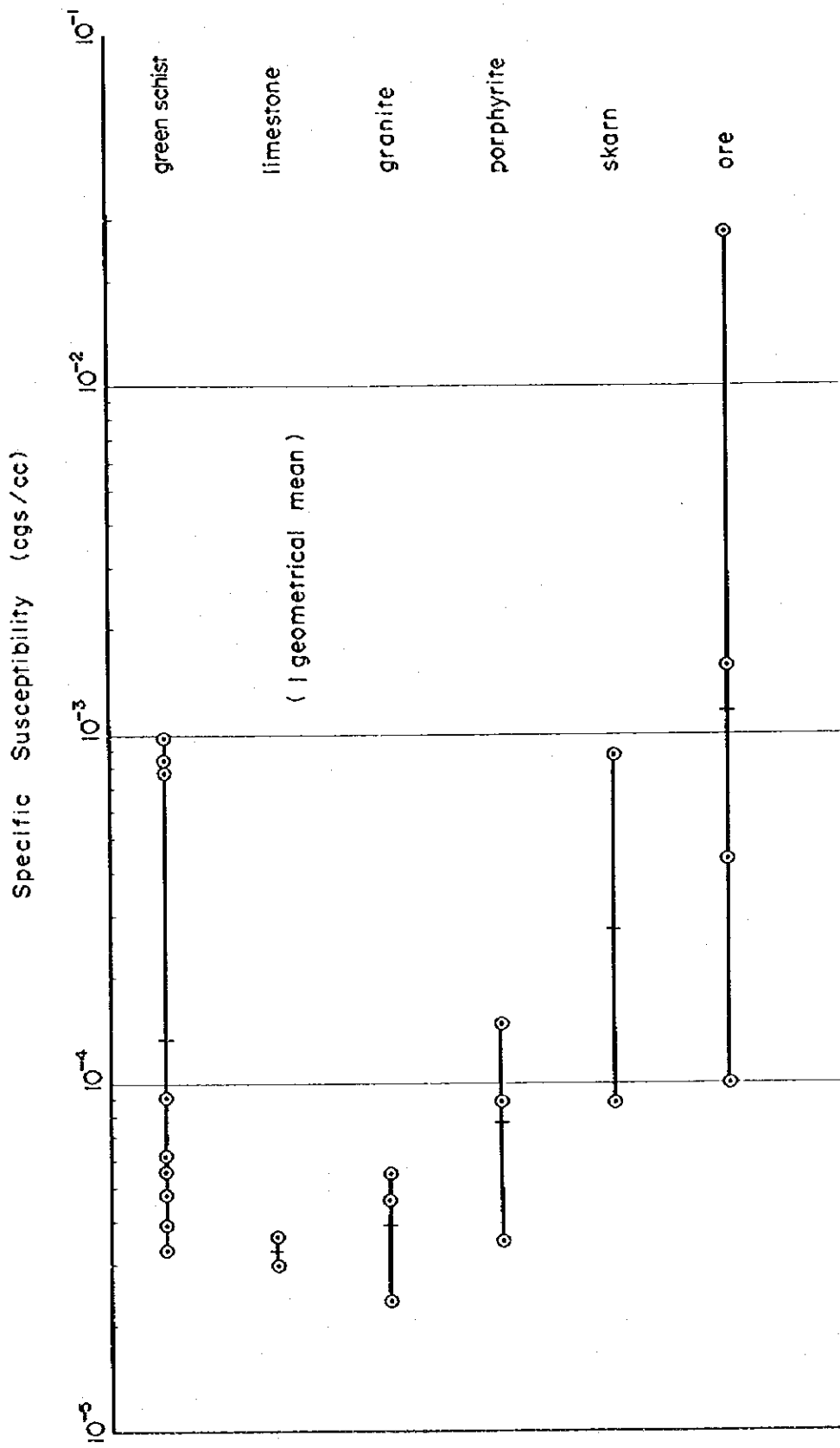


Fig. II-1-7 Results of Magnetic Susceptibility Measurements

4) Ores present high magnetic susceptibility in average, though the variation of their measured values is high.

Detected susceptibility of ores
(100 to 27,400) $\times 10^{-6}$ cgs/cc
average susceptibility
1,169 $\times 10^{-6}$ cgs/cc

Although the numbers of samples are limited, the aforementioned results are reasonably thought to indicate the tendency of magnetic susceptibility of rocks in the survey area. Anyway, granite shows as low magnetic susceptibility as that of limestone, suggesting that the granite of the survey area belongs to low magnetic mineral bearing type. There are three kinds of schists, that is, pelitic, psammitic, and conglomeratic types, and in particular case of conglomeratic type, the contained amount of magnetic minerals presumably differs very much depending on the kind of gravels/boulders in the conglomeratic schists. And then it is naturally considered that there are two groups, as a whole, of both low magnetic susceptibility and high susceptibility.

1-3 Discussion

1-3-1 Relations between Survey Results and Mineral Indications

1) East grid survey area

There are several skarn zones extended from north to south for about 2,000 m in the limestone distributed area, and some part of the zones being mineralized with occurrence of ore minerals such as chalcopyrite and pyrrhotite. In particular, relatively strong mineralization was recognized in the area on both side of the river which flows near the Agadir village down toward the east.

In reviewing the total magnetic intensity map (Pl. II -1-2), numbers of medium amplitude (approximately 100 nT to 200 nT) anomalies with short wavelength (50 m to 100 m in diam.) were recognized extending for about 1,500 m from north to south with their centers located at around the Agadir village in the limestone distributed area. Of the skarn distributed area, both the north and the central parts nearly correspond with the above mentioned magnetic anomalous area. Particularly, in the north to south elongating zone of 300 m which has its center at the Agadir village, the magnetic anomaly almost coincides with the mineralized skarn zone.

Results of the model calculation suggest that those anomalies could be explained by a model of intruded rock bodies with magnetic susceptibility of around 10^{-3} cgs/cc, where the rock bodies being assumed coming close to the surface. In other words, it can be inferred that the magnetic anomalies occurred in the low susceptibility limestone wherever skarns with much magnetic minerals exist in abundance.

On the other hand, in the southern part of the survey area, there is a narrow distribution of skarn zones. However, magnetic anomaly is weak there, and the correspondence with the skarn zone is not clear. From these facts, the skarn zone in the south could be inferred small in scale deep in the ground as well as on the ground, and the possibility of the mineralized zone which is rich in magnetic mineral might be low.

2) West grid survey area

In the west grid area, schists are widely distributed, and numbers of granitic intrusions are found in small scale in the area. In some part of the schists, minor vein type ore deposits have been formed which contain such ores as chalcopyrite, pyrrhotite, etc.

In the area, just the same as in the east area, plenty of short wavelength magnetic anomalies of 100 nT class are observed. These anomalies do not always correlate with the mineral indication zone which are found on the surface. According to the IP survey results, which will be explained later, the current survey area is generally low in FE effect except the north eastern part, and no particular indications suggesting the existence of a large scale mineralized zone have been found as yet. Consequently, there is a possibility that the magnetic anomaly of the area has a correspondence either with the high magnetic materials related with a weak mineralization observed in the area or with a highly magnetized rocks in the schists.

In addition, there is a long wavelength magnetic anomaly in the mineral indication zone which is located from the western edge to the southern part of the area. And a magnetic distribution which coincides with the elongated direction of the vein can be observed, and this suggests that the said distribution probably reflect the structure of the schists.

3) Other than the grid survey area

As previously mentioned, there are four major magnetic anomalies distributed with larger wavelength and amplitude in the captioned area which also include the anomaly located at the southern end of the west grid survey area. These anomalies are to be explained, according to the results of a model calculation, that a high magnetic body of 10^{-3} cgs/cc or so would be located at relatively shallow depth with its width over 150 m. As explained already, the known ore deposits are either skarn or vein types in the current survey area, then it is not likely that each of their mineralization zones has such a wide width obtained by the model simulation. From this fact, it is duly considered that the said magnetic anomalies have little possibility of being related with the mineralization zone. The cause of the magnetic anomalies are probably to be considered arisen by, (1) the presence of large scale hidden intrusives with high magnetic susceptibility (2) collected distribution of high susceptibility rocks in the schists.

Other anomalies observed are all small in scale, and it is hard to assume for a high magnetic susceptibility zone like skarn zone, namely a magnetic rock body, being well developed in the captioned area. It is to be judged that this area is rather uniform in magnetism as a whole.

1-3-2 Relations of Magnetic Distribution and Rocks Type

The relation of the magnetic distribution with major rock members has been summarized, and is shown in Table II-1-3.

Table II — 1 — 3 Relation between Change of Magnetic Intensity and Geology

Rock Type	Geological Distribution	Magnetic Distribution	Susceptibility K	Remarks
Schists	Green schist (conglomeratic) Psammitic schist Pelitic schist	Large scale anomalies in four localities. Numbers of short wavelength anomalies	low and high	Intrusives with large K in the depth. Schist with large K. Mineralization?
Limestone	Distributed from N to S in direction, to the east of schists	Almost no anomaly Small gradient in magnetic intensity	low	Uniform K value nearly equivalent with surrounding formations?
Skarn	Limestone distribution area	Anomalies of short cycles in abundance	high	Pyrrhotite
Granite	Large rock body in the west Stocks in the east Numbers of dyke intrusives	Almost no anomaly Small gradient in magnetic intensity	low	K value nearly equivalent with surrounding formations
Porphyrite	Northwest, Northeast, and Southeast, distributions in small scale	Almost no anomaly (except southeast)	medium	Small scale rock bodies? K value not much different from surroundings?

There is a large directional trend from NE to SW regarding iso-magnetic intensity contours in the survey area (PL. II-1-2 to PL. II-1-5). This trend and the distribution of limestone coincide well in the north to central part of the survey area, however in the southern area they do not coincide each other. Instead, there is a tendency reflecting the strike of schists in the southwestern area, and this suggests a possibility that there is a change in regard to the ruling factors on the magnetic distribution.

1-3-3 Summary

1) The regional magnetic distribution has a general continuity in north to south direction, and looks concordant with the regional geological structures of the survey area.

2) The regional trend of the magnetic distribution shows high magnetic intensity in the east, and this fact suggests the predominance of magnetic rock bodies there in the eastern area.

- 3) There are two types of magnetic anomalies in the survey area, that is,
A) Anomaly with long wavelength and large amplitude
B) Anomaly with short wavelength and medium amplitude.

4) Type A) anomaly has been recognized in four localities all of which are in schist distributed areas, and it seems to have less direct relations with the mineralization zones. Consequently, it can be inferred that the A) type anomaly reflect a large hidden intrusive mass with high susceptibility or high magnetic susceptibility rocks in the schist.

5) Type B), which is mentioned item 6) and 7), has been found in the east and southwest parts of the survey area.

6) The anomaly of the east has been found much in the zone which likely has its center at the Agadir village extending for about 1,500 m from north to south. Its dimension in E-W direction approximately coincides with the limestone distribution. The magnetic anomaly distribution reflects the distribution of skarns, particularly around the Agadir village where the magnetic anomaly nearly corresponds with the mineralized skarn zone. According to the model simulation, a dyke shaped magnetic body with high magnetic susceptibility has been inferred, and correlated with the skarn. In the south of the said anomaly, magnetic anomalies become small in scale, and no indications have been obtained which suggest a predominant mineralization zone rich in magnetic minerals.

7) Magnetic anomalies in the southwest are all located in the schists distributed areas. Correspondence of the anomaly location with the discovered ore vein on the surface has not been fully clarified. The areal magnetic anomaly may be correlated to either some highly magnetic materials holding a relation with weak mineralization or some rock in the schists which has a high magnetic susceptibility. In addition, no indications suggesting the existence of large scale mineralization have been obtained from the IP survey results.

8) Magnetic anomalies have been scarcely found which can be corresponded with the distribution areas of either granite or porphyrite.

9) Regarding the survey results of magnetic susceptibility, limestone and granite have been found equally low, then porphyrite, skarn, and ores have followed in becoming higher susceptibility in this succession. On the other hand, susceptibilities of the schist have shown two types, where there are the one with susceptibility as low as limestone, and the other group with higher susceptibility nearly equivalent with that of ores.

10) In case when the skarn zone exists in either limestone or granite as it is in the eastern part of the survey area, the contrast of magnetic susceptibility becomes large, and it makes the magnetic survey more effective in the field.

CHAPTER 2 IP SURVEY

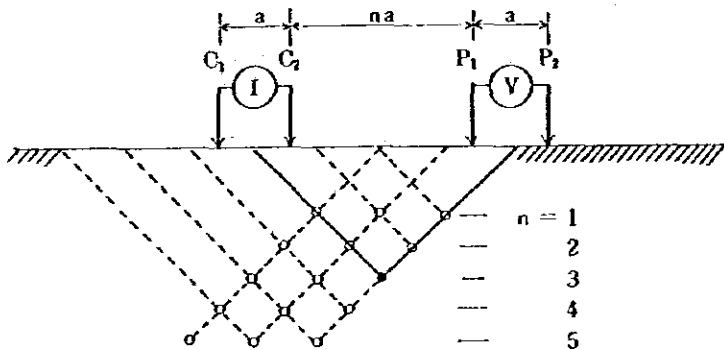
2-1 Outline of IP Survey

2-1-1 Outline of IP Method

The induced polarization method is an electrical prospecting technique based on the phenomenon of induced polarization (IP) which is an electro-chemical polarization that occurs across an interface between the electron-conducting mineral and the pore solution. In addition to resistivity values, an IP survey measures the IP effect that is caused by IP phenomenon. Every mineral and rock show IP effect, although with widely different degree depending on the type of such mineral or rock. In general, a strong IP effect is found on chalcopyrite, pyrite, chalcocite, pyrrhotite, galenite, and other sulfide minerals as well as magnetite and graphite.

Two modes are available for IP measurement: the time-domain mode and the frequency-domain mode. Our survey used the frequency-domain mode. It measures the difference of apparent resistivity between two different frequencies so that an IP effect is estimated in the form of a frequency effect value. Generally, a frequency effect (FE) value increases with an IP effect level.

A schematic figure below shows a dipole-dipole electrode configuration used in this survey.



a: Electrode Spacing (50m)

n: Electrode Separation Index (1 to 5)

C₁, C₂: Current Electrodes

P₁, P₂: Potential Electrodes

Dipole-Dipole Configuration

Apparent resistivity values and FE values are calculated by the following equation:

$$\rho_h = K \cdot \frac{V_h}{I}$$

$$\rho_l = K \cdot \frac{V_l}{I} = \rho_h \left(1 + \frac{FE}{100} \right)$$

$$FE(\%) = \frac{\rho_l - \rho_h}{\rho_h} \times 100 = \frac{V_l - V_h}{V_h} \times 100$$

where,

- I : transmitting current
- ρ_h : apparent resistivity for high frequency
- ρ_l : apparent resistivity for low frequency
- V_h : potential difference for high frequency
- V_l : potential difference for low frequency
- FE : frequency effect
- K : geometric constant, $K = \pi a n(n+1)(n+2)$

2-1-2 Field Survey

1) Survey line setting

The area of IP survey is 2 km by 2 km, as illustrated in Fig. II-2-1, covering the southern half of the magnetic survey area. Elevation of the IP survey area ranges from 1800 m to 2500 m above sea level, mostly comprising steep mountaneous slopes.

After examing the results of geological and magnetic surveys, we designed survey lines with inspector's approval so as to effectively cover those areas where skarn and mineralization were most likely to be found. Thirteen survey lines were set in an area where skarns were distributed in the eastern part of the survey area, and other 6 lines were set in the western part of it where mineralization was observed in schists. All the survey lines run in the east-west direction. For these lines, existing survey lines which have been set for a previous geochemical survey, were used and were extended, if necessary, by 150 to 200 m from both ends of individual lines by a transit-compass. The survey lines were arranged in parallel at an interval of 100 m and 200 m, and survey stations were set at every 50 m in horizontal distance along each line.

Survey lines and stations are as follows:

Line name (Line No.)	Line length (km)	Number of stations
1	0.8	17
3	0.8	17
5	0.8	17
7	0.8	17
8	0.8	17
9	0.8	17
10	0.8	17
11	0.8	17
12	0.8	17
13	0.8	17
15	0.8	17
16	0.8	17
18	0.6	13
21	0.8	17
22	0.8	17
23	0.8	17
25	0.8	17
27	0.8	17
29	0.8	17
Total	19 lines 15.0 km	319 stations

2) Outline of measurement

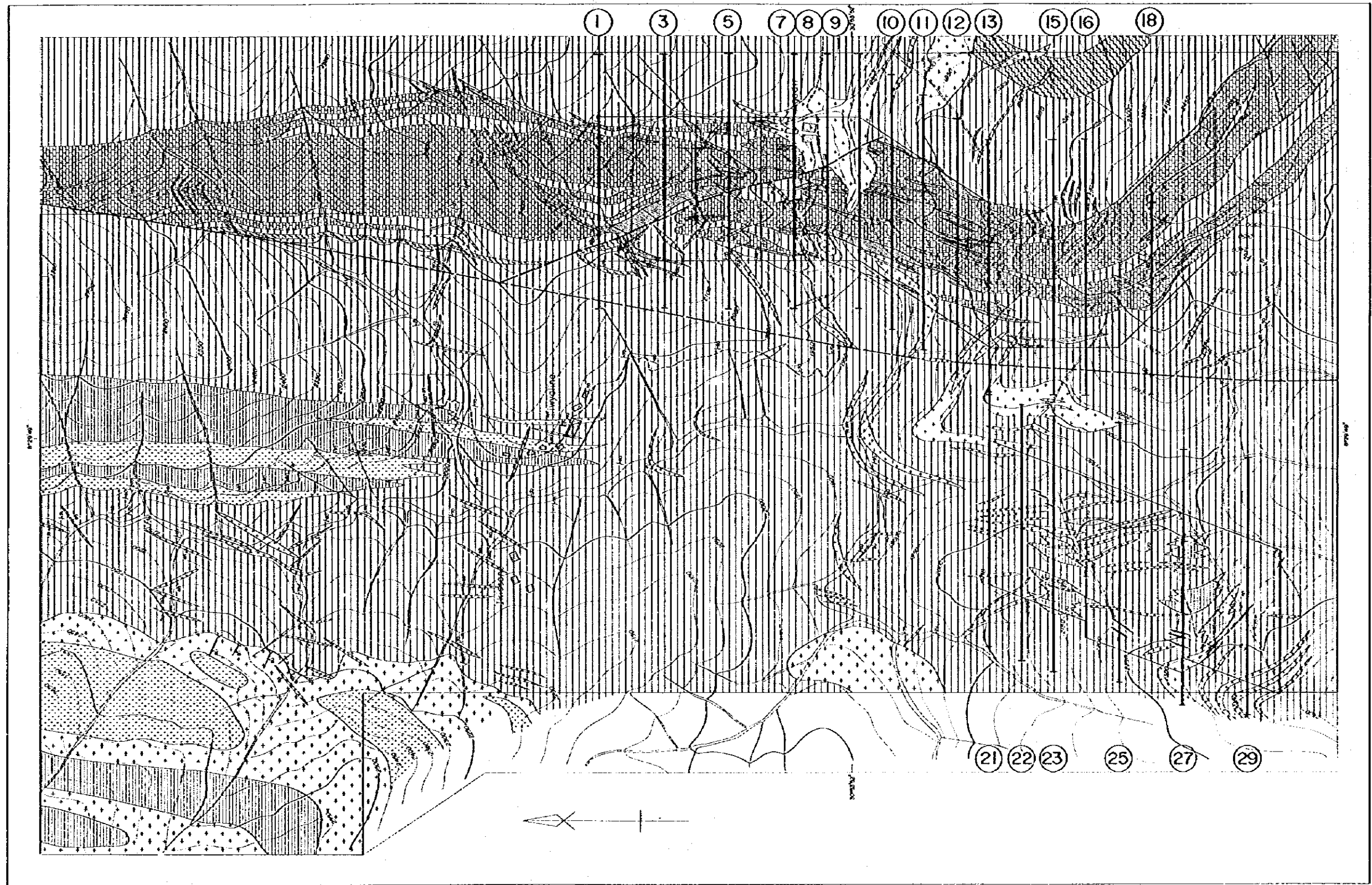
A brass plate of 30 cm by 30 cm was used as a current electrode, which was buried in soil about 50 cm below surface. Mixture of water, salt and bentonite were poured between an electrode and surrounding soil in order to lower grounding resistance.

For measurement, a transmitter was installed approximately at the center of each survey line, and a receiver was shifted appropriately along each survey line. Amperage of the transmitting current was about 0.1 to 0.5 A.

3) Equipments used for the IP survey were as follows:

(1) Transmission

- Transmitter: MI 5609 AB model, Yokohama Electronics Lab.,
maximum output 800V, 1A.



LEGEND

- | | | | |
|--|-----------------------------------|--|------------|
| | green schist (tuff, tuff breccia) | | granite |
| | pelitic schist | | porphyrite |
| | psammitic schist | | skarn |
| | limestone | | fault |
| | calcareous schist | | ore vein |

① Line number
 | IP Survey line

S=1:12,500
 0 500m

Fig. II-2-1 IP Survey Area with Survey Lines

- Motor generator: EG 800F model, Shindaiwa Co., output 0.8 kW, 60 Hz.
 - Current electrode: 30 cm by 30 cm, brass plate.
- (2) Reception
- Receiver: DF 58Z model, Yokohama Electronics Lab., sensitivity 1 μ V.
 - Potential electrode: copper-copper sulfate non-polarized electrode pot.

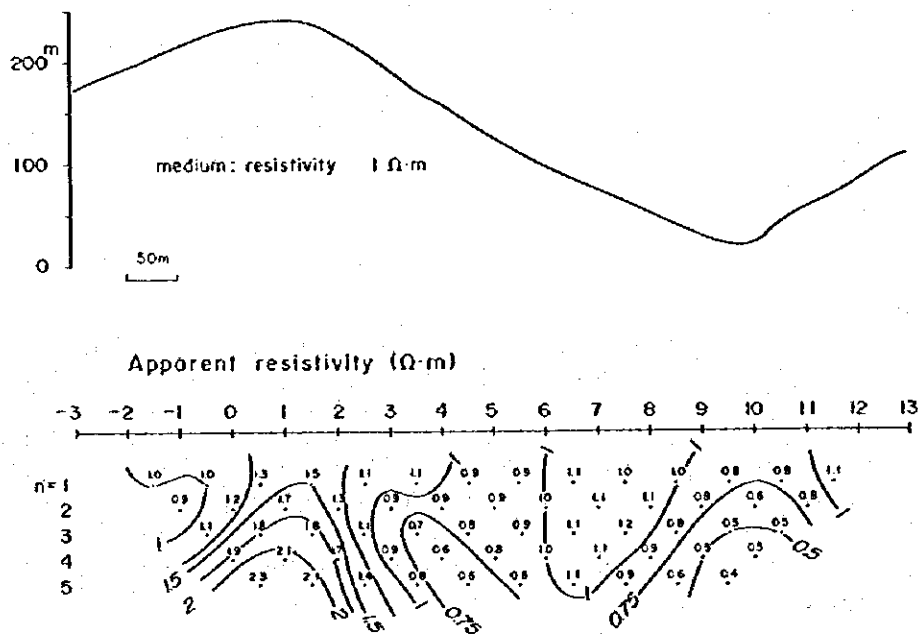
2-2 Results of IP Survey

2-2-1 Effects of Topography on Apparent Resistivity

In general, apparent resistivity, measured at rugged terrain such as mountain ridges and valleys is subject to the effects of topography, which must be taken into account for interpretation of such measurements. In our survey, topographical effects were estimated by calculation with a following two dimensional model (the relief shown in the following figure extends perpendicular to this figure). The figure illustrates changes of apparent resistivity of rock formations having a uniform resistivity of 1 Ω m, due to topography and shows the following features:

1) A zone of high apparent resistivity appears underneath a mountain ridge, and two low apparent resistivity "roof-shape" zones appears its both sides, each of such low zones with dipping both east- and westward.

2) A low apparent resistivity zone appears underneath a valley, and two relatively high apparent resistivity roof-shape zones appears its both sides.



Topographical Effect on Apparent Resistivity

2-2-2 Distribution of Apparent Resistivity and FE along Individual Survey Lines (See Fig. II-2-2 to Fig. II-2-20.)

1) Line 1

Apparent resistivity values, hereafter called as AR, range from 1 to 8 k Ω m. By removing topographical effects, most of the values can be reduced to a few k Ω m. The effects of topography are obvious in the high AR zone around Station 3, and in the low zone around Station 8.

FE values, hereafter called as FE, are within a range between 0.7 and 2.0%, averaging about 1.2%. Generally FE are low and monotonous. No anomaly of FE was observed along this line.

2) Line 3

AR are generally high, varying between 1.4 and 12 k Ω m. Again along this line, a high AR zone around Stations 3 to 5, and a low zone around Stations 9 to 11 are presumably influenced by topography.

FE, ranging from 0.9 to 2.7%, are mostly as low as 1.5% or less. Slightly higher FE are found around the west end of the line and around Station 6, but they are not high enough to be regarded as FE anomalies.

3) Line 5

AR are between 0.7 and 11 k Ω m and somewhat lower than those along Lines 1 and 3. A high zone of AR around Stations 4 to 6, a low zone around Station 3, and another low zone around Station 10 are presumably due to the effect of topography.

FE are within a range of 0.7 to 3.0%, but mostly less than 1.5%. A zone of over 2% FE are found in the western part of the line (Stations 0 to 2), and perhaps this is an extension of the above-said slightly higher FE at the west end of Line 3.

4) Line 7

AR along this line vary from 0.5 to 11 k Ω m. Two low zones of 1 k Ω m are found, one having a crest around Stations 0 and 1 and dipping eastward, and another around Station 8. The effect of topography appears as each low zone around Station 1, Station 8 and Station 9 as well as in a high zone around Stations 3 to 6. Among them, the low zone around Station 1, after reducing effect of topography, is still low.

FE are within a range of 0.4 to 4.1%. A relatively high FE zone of 2 to 4% is found in the western part of this line, with its crest around Station 1 and dipping eastward. This anomaly extends from northern survey lines, and corresponds with a low AR zone. Most other parts of the line show low FE between 1 and 2%.

5) Line 8

AR vary between 0.1 and 13 k Ω m. A roof-shape zone of low apparent resistivity of 0.5 k Ω m and less is observed, with Stations 3 and 4 crest. This zone and another such zone along Line 9 show the lowest values of AR in the whole of the present survey area. Even after reducing effect of topography, AR along this line is the lowest in the survey area.

FE vary widely between 0.9 to 8.5%. In an area from Stations 1 to 5, FE in near surface are as high as 4% or more. Moreover, a high FE zone of roof-shape is found, with Stations 3 and 4 as a crest, and this zone corresponds with low AR. At Station 3, FE in the depth are as high as 4 to 5%, and this anomaly may be an extension of similar ones in northern survey lines.

6) Line 9

AR range between 0.1 and 9.8 k Ω m. A roof-shape low AR zone of 1 k Ω m or less is observed with Stations 2 to 5 as a peak.

FE distribute somewhat widely, ranging between 1.5 and 5.9%. A roof-shape high FE zone of 4 to 5% is found, with Stations 3 to 5 as a crest.

The lower part of Stations 3 and 4 shows low FE, and this anomaly also is probably an extension of anomalies in the adjacent northern survey lines.

7) Line 10

AR are highly various ranging from 0.2 to 36 k Ω m. High values in AR are found around Stations 5, 8 and 11, and a comparison with Lines 7, 8 and 9 in the north suggests that these values are influenced by topography. However, a general trend in AR of this line is still higher than those of adjacent northern lines. The values around Station 3 are 1 k Ω m or less.

FE are as high as 4% or more in the depth of Stations 1 to 3, and in a zone having a crest at Stations 2 and 3 and dipping eastward. FE are 2 to 3% in the west side of Station 1, and also in the depth of Stations 5 to 10. Around further eastern stations, FE are as low as 1 to 2%, and this anomaly may be an extension of those of the north lines.

8) Line 11

AR are generally lower in the west side, and higher in the east side of Station 5. High AR are observed around Stations 6 and 9, due to topographical effects. In general, highland in the east show higher AR, and lowland in the west lower AR. In addition, a roof-shape zone of 1 k Ω m or less lies, with its crest around Station 2.

There is a roof-shape zone of FE 4 to 5%, with Station 2 as its crest. This zone coincides with AR distribution. A low FE zone lies underneath this high zone. An extensive zone of low FE between 1 and 2% spreads around Station 5 and further eastern part of this line.

9) Line 12

AR range widely from 0.3 to 80 k Ω m. A low AR zone of 1 k Ω m or less is found in the middle and lower parts underneath Stations 6 and 7, although presumably this is influenced by topography.

High FE zone of 4% or more are found around Stations 6 and 7 as its crest and dipping westward. The circumference of this zone as well as the depth of Stations 2 to 6 shows FE between 3 and 4%. This FE anomaly also corresponds with a low AR zone, and is presumed to be an extension of anomalies of northern lines all having their common nature. Station 9 and further eastern part of the line show a low FE ranging from 0.4 to 1.7%.

10) Line 13

AR are generally higher than those of northern lines where FE anomalies are observed. For the Electrode Separation Index $n=1$ to 4 an extensive zone of 5 k Ω m or more is observed beneath the Stations 3 to 10. In other parts of the line, AR are between 1.5 to 5 k Ω m.

The depth of Stations 6 to 8 shows FE above 3%, and its circumference shows FE between 2 and 3%. This FE anomaly also corresponds with relatively low AR suggesting that it may be an extension of a northern zone of anomaly, although it is weaker than the northern one. An FE zone of between 2 and 3% is observed, with Stations 0 to 2 as its crest and dipping eastward.

11) Line 15

AR at Stations 2 and further westward are relatively low, ranging between 1.5 to 3.8 k Ω m. In most of the eastern part of the line beyond Station 2 AR are high at 5 k Ω m or more.

FE are mostly as low as 0.7 to 1.8%. Only a zone covering Stations 0 to 2 shows 2% or more, but it is too low to be called as an anomaly.

12) Line 16

AR at Station 4 and further east are mostly as high as 5 k Ω m or more. Even after topographical effect is taken into account, this AR is still high. However, a low AR zone of 2 to 4 k Ω m is found around Station 1 in the west.

FE around Station 3 and further western part of the line are slightly high at 2.1 to 3.4%, but all the values in the east side of this station are

as low as 1 to 2%. On this line again, higher FE are found in a zone of relatively low AR, but these are not anomalous FE.

13) Line 18

AR at most of the stations are high, at 5 k Ω m or more.

FE of over 2% were observed at a few points in the depth beneath Stations 0 and 1. Except these, all FE are between 1 and 2%. No FE anomaly is found.

14) Line 21

AR at nearly all stations are high, showing 2 to 9 k Ω m. A high AR around Station 2 is presumably influenced by topography.

FE are 2% or more at Station 7 and further eastern part of the line, and also in the upper part (n=1 and 2) of Stations -1 to 2. Some parts of these zones are slightly over 3%, showing somewhat high FE. All other parts of the line shows low FE ranging from 0.6 to 1.9%.

15) Line 22

AR at most stations are within a range of 2 to 9 k Ω m. High AR around Stations 3, 8 and 11 are perhaps influenced by topography.

FE are 2% or more at a number of stations east from Station 7, including some 3% or higher values. This higher FE is probably an extension of the high FE zone in Line 21 in the north.

16) Line 23

AR are mostly 2 to 5 k Ω m. High AR are found around Stations 1, 7 and 9 may be under the influence of topography.

FE of as high as between 3 and 4% are found around Station 8 as a crest and dipping eastward, suggesting that this high zone is an extension of high zones in northern adjacent lines. FE around Station 7 and all the further eastern part are between 2 and 3%, and almost all of them in the west side of that station are between 1 and 2%.

17) Line 25

AR are high all over the line at 2 k Ω m or more. Because of topographical effects, high AR are found around Station 6, and also around Station 11.

FE are mostly between 2 and 3%, and no anomalous zone is found.

18) Line 27

AR are high all over the line at 2 k Ω m and higher. Presumably due to topographical effects, high AR are found around Station 1, and also in a zone covering Station 6 and all the further eastern part of the line.

FE range between 0.4 and 3%. Zones of slightly higher FE between 2 and 3% are found at the near surface of Stations 1 to 4, and in the depth of Stations 6 to 10, but these are not to be regarded as anomalous FE zone.

19) Line 29

AR in a fairly sizable zone in the depth of Stations 2 to 4 are somewhat low, at 2 k Ω m or less. Except this, the most part of the line have values of 2 k Ω m or more. Presumably due to topographic effects, high AR is observed around Stations 8, 9, and all stations from Station 12 eastward to the end.

FE of Stations 5 to 12 are between 2 and 3%. In all other parts of the line, FE are low, between 1 and 2%. No anomalous zone is found.

2-2-2 Plan Distribution of AR (See PL. II-2-2 to PL. II-2-11)

1) For electrode separation index n=1

(1) A zone of low AR at 1 k Ω m or less extends continuously across the western part of all Lines 7 through 11. The width of the zone is 50 m (for Lines 7, 10 and 11) to 200 m (for Lines 8 and 9) in the east-west direction, and about 400 m in the north-south direction. The central part of the zone is a lower AR of 0.5 k Ω m or less. Moreover, another zone of 1 k Ω m or less

AR covers Stations 8 to 10 of both Lines 7 and 8 (the Agadir village).

(2) A slightly wide zone of 1 to 2 k Ω m is found surrounding the low AR area outlined in the paragraph (1) above, and in particular around the Agadir village.

(3) All other area (viz. most part of the survey area) shows AR of 2 k Ω m or more. It is remarkable that extensive zones of high AR of 5 to 10 k Ω m are observed in the eastern highland part of Lines 9 to 18 and also in the eastern part of Lines 27 to 29.

2) For electrode separation indices n=2 to 5

(1) The low AR zone of 1 k Ω m or less, which is found for n=1, is still observed for n=2 to 5, in some more expanded or contracted shape. However, for n=3 to 5, a part of this low zone is split, forming independent low AR zone around Stations 6 and 7 of Lines 8 and 9. Another low AR zone around the Agadir village has disappeared.

(2) A wide zone having AR of 1 to 2 k Ω m surrounds the low AR zone outlined in Paragraph (1) above. This relation between two zones is similar to the relation found in the case of n=1, although this zone is now narrower around the village. (Presumably, the low AR observed for the case of n=1 is due to the existing cultivated land.)

2-2-3 Plan Distribution of FE (See PL. II-2-12 to PL. II-2-16.)

1) For electrode separation index n=1

(1) Zones of high FE of over 4% is observed around Stations 2 to 5 of Line 8, around Station 5 of Line 9, around Stations 3 to 4 of Line 10, and around Station 2 of Line 11. Widths of these high FE zones are wider along Line 8 (150 m), and narrower along Line 11 (50 m). Furthermore, a zone of a relatively high FE of over 3.5% is observed, covering Stations 5 and 6 of Line 12 and a part of Line 13.

(2) A zone of slightly high FE of about 3% is found in the eastern part of Lines 21 to 23.

(3) A zone of between 2 and 3% FE surrounds the high FE zone outlined in Paragraph (1) above, and another 2 to 3% zone is found extensively from Lines 21 to 29.

(4) All the remainder of the survey area has low FE of 2% or less.

2) For electrode separation indices n=2 to 5

(1) The high FE zone of about 4% or more, which is observed at n=1, continues downward (n=2 to 5), except that for n=4 and 5 a low FE zone lying across Lines 8 and 9 separates this high zone into two parts.

(2) The zone of slightly over 3% FE for n=1, surrounding the above-said high FE zone, is also observed for n=2 to 5, but it further expands both eastward and westward, as compared with n=1. The zone of about 3% FE at the east end of Lines 21 to 23 at n=1 still continues to n=5 with some expansions and contractions.

(3) A high FE zone around the Agadir village has a general trend of north-south extension. However, this high FE zone are divided into the following three independent FE zone.

- High FE zone, extending from Line 8 to Line 9 (around Stations 2 to 5).
- High FE zone, extending from Line 10 to Line 11 (around from Stations 3 and 4 to 6).
- High FE zone, extending from Line 12 to Line 13 (around Station 6).

(4) Relatively high FE zones of 3 to 4%, observed at eastern parts of Lines 21, 22 and 23, are thought to be connected with each other, and showing the north-south weak anomaly.